Thermochimica Acta, 228 (1993) 379–392
Elsevier Science Publishers B.V., Amsterdam

Thermal decomposition of caesium permanganate

Andrew K. Galwey * and Seham A.A. Mansour [1]

School of Chemistry, The Queen's University of Belfast, Belfast BT9 5AG, Northern Ireland (UK)

(Received 15 February 1993; accepted 7 April 1993)

Abstract

A kinetic study of the thermal decomposition of caesium permanganate confirms previous observations by P.J. Herley and E.G. Prout (J. Chem. Soc. (1959) 3300). Our scanning electron microscope, high magnification examination of the textures of product and of partially decomposed samples provides evidence that reaction is accompanied by melting. Accordingly we here reconsider the reaction mechanism and conclude that anion breakdown proceeds through electron transfer between anions

$2MnO_4^- \rightarrow MnO_4^{2-} + [MnO_4] \rightarrow MnO_4^{2-} + MnO_2 + O_2$

within a local intracrystalline molten phase resulting from fusion of a ($CsMnO_4 + Cs_2MnO_4$) eutectic.

INTRODUCTION

The study of the thermal decomposition of potassium permanganate by Prout and Tompkins [1] has been widely regarded [2] as one of the earliest solid state reactions for which a detailed reaction mechanism was provided. This article is associated with the provision of a theoretical interpretation for the solid state rate expression now usually referred to as the Prout–Tompkins equation

$$\ln(\alpha/(1-\alpha)) = kt \qquad (1)$$

where α is the fractional reaction. This paper was followed by similar kinetic studies of the decompositions of caesium permanganate [3] and of rubidium permanganate [4] and the influences of preirradiation on these and related thermal decompositions [5]. The thermal reactions of both $CsMnO_4$ and $RbMnO_4$ obey eqn. (1). The deceleratory period of $CsMnO_4$

* Corresponding author.
[1] Permanent address: Department of Chemistry, Faculty of Science, Minia University, El Minia, Egypt.

breakdown was relatively short (estimated to occur $\alpha > 0.7$ [3]) and the early part of the reaction of whole single crystals of the same salt obeyed the power law [2] with $n = 2$

$$\alpha^{1/2} = kt + c \tag{2}$$

Since these studies, an extensive literature concerned with the thermal reactions of $KMnO_4$ has appeared [2] but relatively very much less attention has been directed to the pyrolysis reactions of the other alkali permanganates. Accordingly we consider it to be timely to undertake a further study of $CsMnO_4$ decomposition and to consider the mechanism in the context of recent advances in solid state chemistry.

In their study of $CsMnO_4$ breakdown, Herley and Prout [3] found that, "it was not possible to follow the decomposition visually", using an optical microscope. They did report, however, that crystals disintegrated prior to the final deceleratory period of reaction ($\alpha > 0.7$). We considered it to be appropriate to exploit the greater resolving power of the scanning electron microscope to investigate whether textural evidence could be obtained concerning the previously proposed decomposition mechanism [3]. In this it was suggested that reaction proceeded through the propagation of cracks into undecomposed material followed by favoured nucleation at or in these cracks. Further investigations of this rate process is of particular interest because the acceleratory phase of $CsMnO_4$ decomposition is unusually prolonged, perhaps to $\alpha > 0.7$ [3].

It was also of interest to consider the chemical steps participating in anion breakdown in the context of the view that $KMnO_4$ decomposition proceeds through electron transfer in the anion sublattice [6]

$$2MnO_4^- \rightarrow MnO_4^{2-} + MnO_4$$
$$\downarrow$$
$$\text{Products}$$

The present study was undertaken, therefore, to reexamine a previously carefully studied reaction, applying modern experimental techniques and interpreting the observations in the perspective of recent theoretical advances in the subject.

EXPERIMENTAL

Caesium permanganate reactant

Caesium bromide (Analar) and potassium permanganate, (0.020 moles of each) were separately dissolved in minimum volumes of distilled water and mixed at ambient temperature. $CsMnO_4$ is sparingly soluble and the precipitate was allowed to stand for 18 h to permit an increase in size of the

relatively small crystallites first formed. This product $CsMnO_4$ was filtered, briefly water washed and dried in the atmosphere. Two identically prepared samples of caesium permanaganate were studied here.

Apparatus

Kinetic studies of $CsMnO_4$ decomposition were based on measurements of the pressure of gaseous oxygen evolved in a conventional glass vacuum apparatus. A weighed reactant sample (about 40 mg $CsMnO_4$), retained in a small glass tube, was evacuated for 30 min at 10^{-5} Torr before isolation from the pumps and admission to the constant temperature (±0.5 K) heated zone. A cold trap (78 K) was maintained between reactant and pressure gauge. The pressure of oxygen evolved in the apparatus was measured at specified time intervals using a MKS Baratron type 222B absolute pressure diaphragm gauge. The outputs from this pressure sensor, together with that of a chromel–alumel thermocouple junction, located in close proximity to the heated reactant, were interfaced with a microcomputer. (Pressure, time, temperature) values were recorded at prespecified time intervals and stored in the computer memory: details of the apparatus have been given elsewhere [7]. Stored measured values were permanently retained on magnetic tape and provision was made in the computer programme for data testing through the fit to those functions of yield α-time that have found application as solid state rate equations [2]. Computed results could be presented for comparative consideration in the form of tabulated data or as graphs.

Electron microscopy

Morphological and textural changes occurring during the course of decomposition of crystalline $CsMnO_4$ were investigated using a Jeol 35CF scanning electron microscope. All specimens were rendered conducting by being coated with a thin Au/Pd film. Samples examined were the reactant (as prepared, $\alpha = 0.00$), the product of the completed reaction ($\alpha = 1.00$) and salt partially decomposed to various appropriate, and measured, α values. Intracrystalline features were exposed by crushing after reaction and comparisons of textures with similarly treated, but uncrushed, salt. The time delay between preparation and sample examination was minimized to avoid deterioration during storage. Many crystals from each specimen were examined and only features identified as being typical, reproducible and significant were photographed. The examples that we have included in the present paper were selected as being entirely representative of the textural changes that occur during $CsMnO_4$ decomposition.

RESULTS AND DISCUSSION

Reaction stoichiometry

From the measured pressures of oxygen evolved in the calibrated volume of the apparatus, on completed decompositions (490–560 K) of known weights of reactant, the mean yield of oxygen was found to be 0.52 ± 0.020 moles O_2 per mole $CsMnO_4$. The mean reactant weight loss ($7.35 \pm 0.15\%$) agreed with expectation (7.52%) for the evolution of one oxygen atom per mole $CsMnO_4$. Titrations of the residual product with standard sodium oxalate solutions showed that <5% MnO_4^- remained after reaction ($\alpha = 1.00$). These measurements are in excellent agreement with the stoichiometric equation

$$CsMnO_4 \rightarrow 0.5O_2 + CsMnO_3 \qquad (\text{or } Cs_2MnO_4 + MnO_2\ [5])$$

The yield on further heating to 700 K was $<0.02O_2$.

This oxygen yield is somewhat less than values reported by Herley and Prout [3] (whole crystals, $0.72O_2$; crushed crystals, $0.67O_2$). Erenburg et al. [8] identify, by X-ray diffraction studies, Cs_2MnO_4 as a solid reaction product.

Electron microscopy

It is useful to present the microscopic observations before discussing the kinetic behaviour. This approach enables the interpretation of rate data to include due consideration of the textural changes that occur in the crystalline reactant during the progress of decomposition [9].

Both preparations of the reactant $CsMnO_4$ included particles of a range of crystallite sizes from approximately $5 \times 5 \times 5\ \mu m^3$ to larger more elongated crystals of approximate dimensions $50 \times 20 \times 20\ \mu m^3$. All were strongly rounded at edges and corners, often giving almost ellipsoid shapes, frequently with one dimension longer than the other two. Surfaces were generally smooth and usually featureless; some of the larger crystals showed areas of flat surface. A typical group of reactant crystallites are shown in Fig. 1.

Soon after the commencement of decomposition a pronounced surface texturing developed which included irregular cracking accompanied by the partial detachment of a thin superficial layer, thickness $<0.05\ \mu m$. A representative texture is shown in Fig. 2 ($\alpha = 0.05$ at 550 K) which includes one of the occasional surface indentations where the disintegration may be identified as the onset reaction. These features were much more obvious when $\alpha = 0.20$ (at 521 K) and are illustrated in Fig. 3 where the crystals selected show areas from which relatively large amounts of material have been detached. Other crystals within the same sample had undergone less disintegration and a few retained most of the original smooth surfaces.

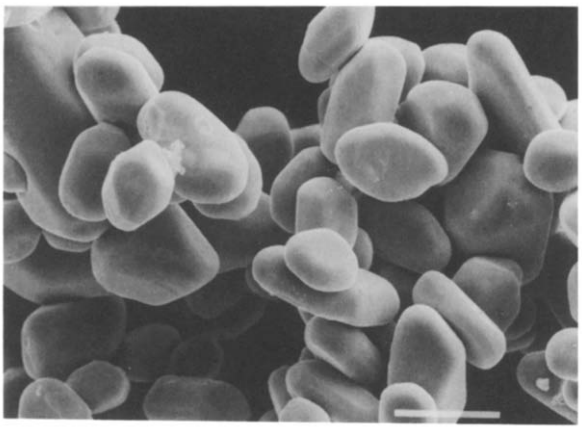

Fig. 1. Electron micrograph of prepared caesium permanganate. Unreacted salt crystals were irregular in shapes and sizes; typically edges and corners were rounded and surfaces were smooth ($\alpha = 0.00$; scale bar, 10 μm).

Within the reorganized intracrystalline material it is difficult to identify features that can be recognized as evidence concerning the mechanism of salt breakdown. We can find no criteria that enable reactant and product to be distinguished. Holes and cracks of various sizes and shapes penetrate the crystal interior which is thereby divided into irregular slabs.

Little further significant textural modification could be discerned between salt decomposed to $\alpha = 0.20$ and material completely reacted ($\alpha = 1.00$) see Fig. 4 (at 502 K). A proportion of the $\alpha = 1.00$ crystals retained their outer, relatively smooth, layer but others, which may have been damaged during handling after reaction, exposed more irregular internal textures. Figure 4(b) shows an irregular internal structure of slabs,

Fig. 2. After the onset of reaction there was some surface retexturing and superficial cracking. The site of damage is regarded as a zone of onset of reaction and only a small number of these features were present in this sample ($\alpha = 0.05$ at 550 K; scale bar, 1.0 μm).

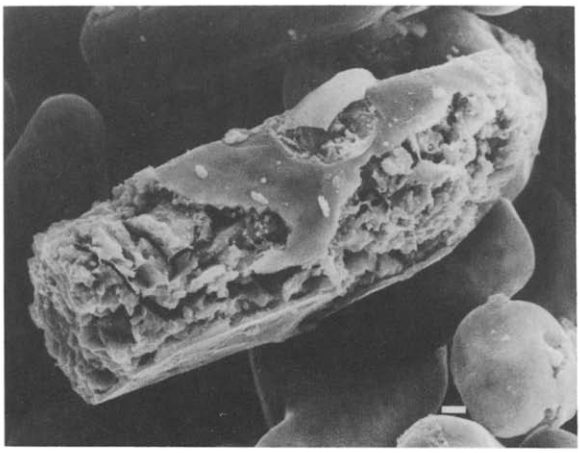

(a)

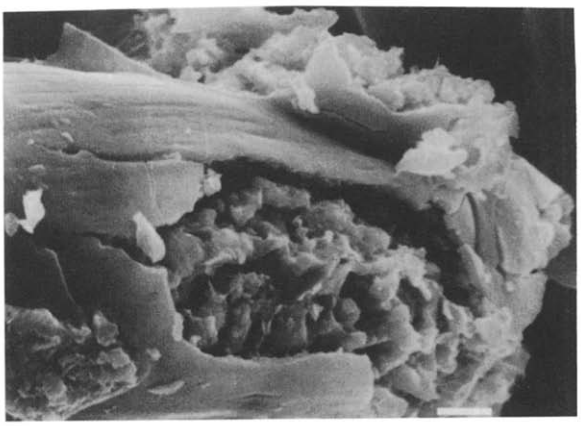

(b)

Fig. 3. (a), (b) At 20% reaction many crystals retained their smooth surfaces but where this had become detached there was extensive internal reorganization, attributed to salt decomposition and selectively revealed in these photographs. No characteristic structures could be recognized in this partially reacted material which can only be described as irregular, penetrated by holes and channels of various sizes ($\alpha = 0.20$ at 521 K; scale bars both 1.0 μm).

Fig. 4. Product of completed decomposition ($\alpha = 1.00$ at 502 K). (a) Some crystals have undergone little, if any, superficial textural change while others have been broken open, possibly during handling, to reveal the irregular textures characteristic of the intracrystalline reaction product (scale bar, 10 μm). (b) A single reacted crystal from which a whole surface has been detached to reveal the irregular, perhaps slab-like, product texture. No regular or aligned crack structure can be discerned (scale bar, 10 μm). (c) The rounded, granular texture of the product which appears to include aggregates composed of smaller particles that have coalesced with sintering or fusion. No regular crack structure can be discerned (scale bar, 1.0 μm).

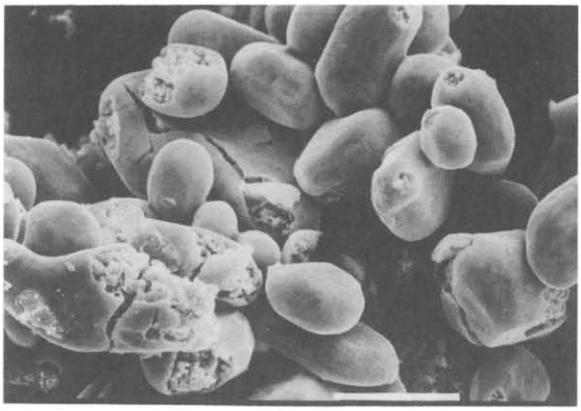

(a)

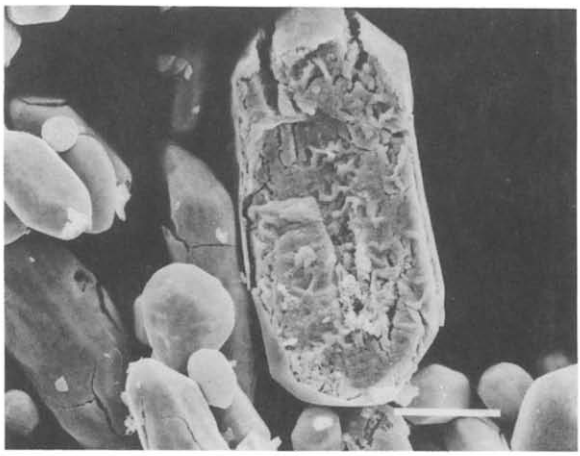

(b)

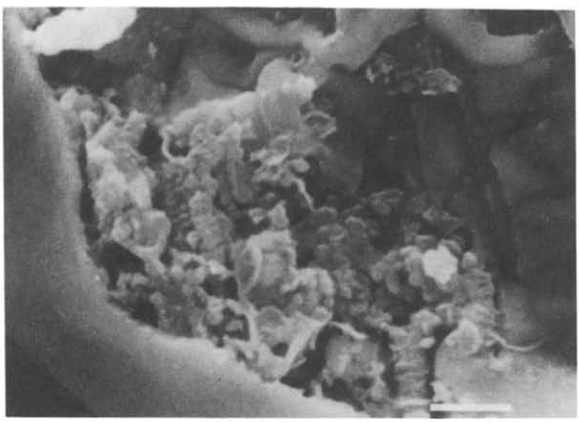

(c)

perhaps with some parallel cracking. At higher magnification (Fig. 4(c)) the product texture shows pronounced irregularity including many rounded particles. There are also indications of sintering and coherent aggregations of locally granular material.

Comment

We conclude, in agreement with the earlier work [3], that reactant crystallites do not undergo comprehensive melting or extensive disintegration during reaction. The early presence of a thin superficial "egg-shell" layer of unreactive, or possibly already reacted, material maintained crystal individualities often to $\alpha = 1.00$. The presence of this layer, enveloping all crystals, and differing in texture from the intracrystalline material beneath it (Figs. 2–4) made it impossible to characterize the progress of modifications occurring during decomposition proceeding within the bulk of the "average" reactant particle. It was not possible, for example, to establish whether reaction developed through the generation and growth of product aggregates or nuclei, and no interface of reactant/product contacts could be recognized. While there was some evidence that reaction was initiated at a limited number of sites, the numbers, sizes and shapes of these could not be characterized. It is also possible that the sizes of nuclei may be below the limits of resolution of our microscope.

The microscopic observations gave no evidence of either extensive or strongly aligned crack propagation within reactant crystals [3]. Intracrystalline product structures were irregular with the appearance of

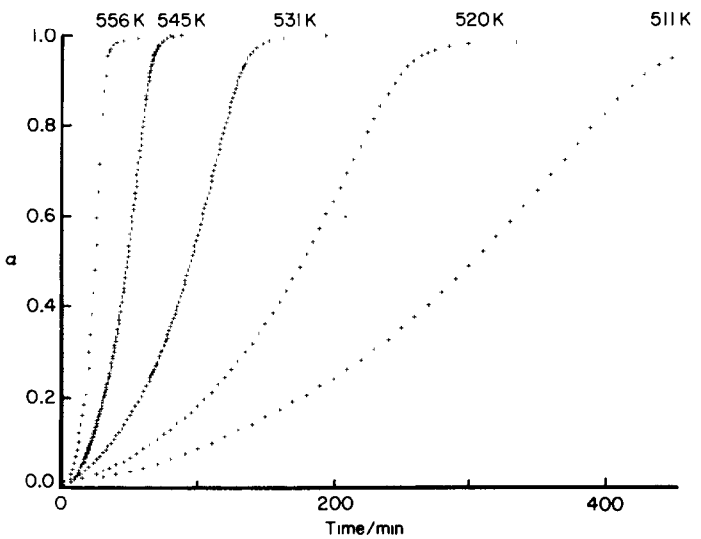

Fig. 5. Typical α-time plots for the isothermal decomposition of caesium permanganate at six temperatures across the range studied.

rounded and granular textures wherein aggregates often appeared to be composed of smaller particles fused or sintered together. While not offering a conclusive proof, the observational evidence is consistent with an intracrystalline mechanism in which reaction proceeds within zones of local, temporary or partial melting, perhaps in a eutectic mixture of manganate and permanganate. Reaction within the fused material is expected to proceed more rapidly than in the more rigid crystal structure [2]. The individuality of particles is maintained by the less reactive particle boundary zone ("skin") as already described for the decomposition of copper(II) malonate [7].

Reaction kinetics

Isothermal measurements of the rate of $CsMnO_4$ decomposition were carried out between 490 and 560 K and representative α-time plots for the oxygen evolution reaction are shown in Fig. 5. As previously [3], the curves are predominantly acceleratory and the best rate equation linear [2] fit found in the present kinetic analysis was the power law, eqn. (2): $(\alpha - 0.02)^{1/2} = kt$, shown in Fig. 6 for the data in Fig. 5. These data were calculated after subtraction of the volume of gas released in a rapid initial process ($\alpha_i = 0.02$) before the onset of the main acceleratory reaction. Very satisfactory linear plots for the eqn. (2) power law (Fig. 6) were found

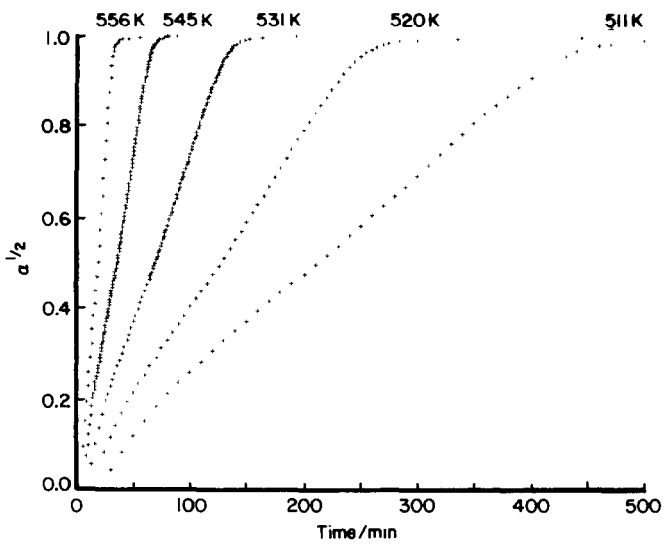

Fig. 6. Power law plots of $\alpha^{1/2}$ against time for the data in Fig. 5. The power law is obeyed $0.03 < \alpha < 0.85$ following a relatively rapid initial oxygen evolution when $\alpha < 0.03$.

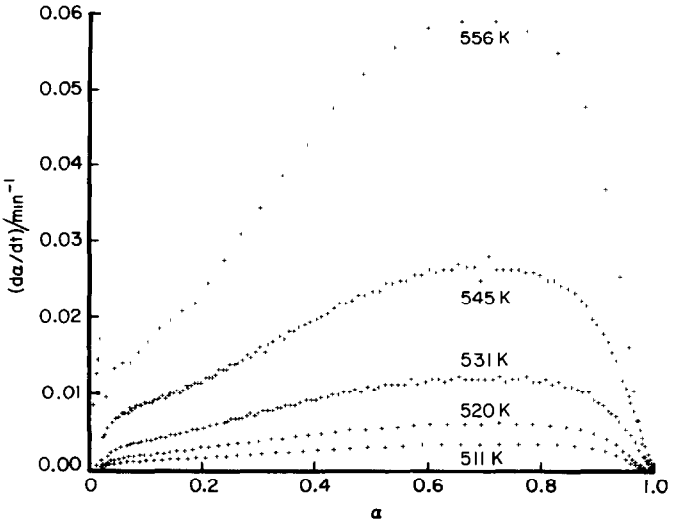

Fig. 7. Differential plots of $(d\alpha/dt)$ against α for the data in Fig. 5.

between $0.03 < \alpha < 0.85$. Differential plots of $(d\alpha/dt)$ against α are shown in Fig. 7 for the same data. Magnitudes of rate constants and the extent of obedience to eqn. (2) measured for the two similarly prepared $CsMnO_4$ reactant samples were virtually identical. From these rate constants we calculate the activation energy for the decomposition of caesium permanganate, in the form of small crystals, as 146 ± 6 kJ mol^{-1}. This compares well with values reported by Herley and Prout [3] of between 140 and 170 kJ mol^{-1}.

Crushed reactant

The kinetic characteristics of the decomposition of reactant crushed in a pestle and mortar were generally similar to the original salt, in agreement with previous observations [3]. One difference found, however, was that the initial rate at low α (<0.2) was relatively greater than that of the prepared salt. The maximum reaction rates, reached when $0.65 < \alpha < 0.80$, were the same as those measured for the prepared reactant. This was unexpected because an increase in surface area of reactant solid often results in a markedly enhanced reaction rate [2]. The decompositions of some crushed samples approximated to constant rate (zero order kinetics.)

Reactant crushed with residual product

Decompositions of mixtures of $CsMnO_4$ crushed with 20% (by weight) of previously reacted salt resulted in a marked enhancement in the rate of the early reaction ($\alpha < 0.1$) and subsequent α-time plots were almost linear. The slight increase in rate between $\alpha = 0.2$ and $\alpha = 0.8$ is shown in the

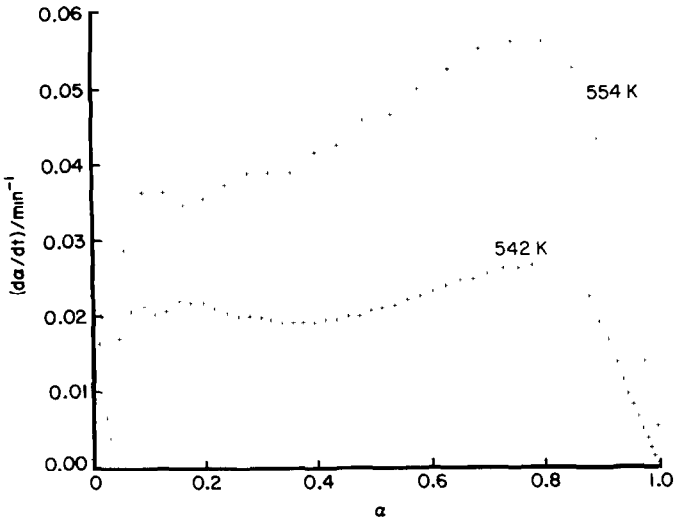

Fig. 8. Differential plots, $(d\alpha/dt)$ against α, for decomposition of $CsMnO_4$ in crushed mixtures with 20% by weight of the solid product from a previous decomposition (at 558 K). These curves should be compared with those in Fig. 7 where the two most rapid rate processes are at similar temperatures. The addition of product accelerates the initial reaction to a rate that increases only slowly between $\alpha = 0.2$ and $\alpha = 0.8$.

differential plots in Fig. 8; these two reactions can be compared with similar plots in Fig. 7 where the two most rapid reactions occurred at similar temperatures. The presence of the product clearly enhances the reaction rate when $\alpha < 0.5$, though it subsequently reaches the same maximum as that found for the prepared salt.

Reaction kinetics for $CsMnO_4$ decomposition in small vapour pressures of water vapour (2–4 Torr) were not detectably different from the reaction of the prepared salt.

The kinetics of decomposition of crushed equimolar mixtures of caesium permanganate and potassium permanganate were, within experimental error, the same as the behaviour of the individual salts alone. There was no evidence of chemical interaction of the salts during these reactions.

Comment

The above kinetic analysis is considered to be incomplete. The extended acceleratory character of the reaction (to $\alpha = 0.65$, see Fig. 7 and ref. 3) is not obviously explained by the electron microscopic observations where the "egg-shell like" superficial layer of crystals obscure the textural changes that accompany reaction. It is also difficult to reconcile the unusually extensive fit to the power law ($n = 2$) (Fig. 6) with a nucleation and growth process proceeding in the asymmetric reactant crystals (Fig. 1). The

absence of an induction period (Fig. 5) is evidence of facile initiation of reaction; nucleation and growth reactions involving rapid nucleation are often predominantly deceleratory [10], which clearly does not apply here. Our data were also shown to give an approximate fit to the Avrami–Erofe'ev equation ($n = 3$) [2], $[-\ln(1-\alpha)]^{1/3} = kt$, between $0.05 < \alpha < 0.7$. This fit is poor both at low α and during the later stages of reaction. The absence of an induction period could be due to previous decomposition of salt during storage (which seems improbable because it was prepared only days before use) or to rapid growth of small nuclei (which is also considered improbable because such behaviour is not found for other salts [2]). We conclude that the kinetic data are not satisfactorily explained by a nucleation and growth reaction mechanism.

In agreement with ref. 3 our data also obey the Prout–Tompkins eqn. (1) (typical plots were linear $0.04 < \alpha < 0.70$, and also followed by a more rapid linear region when $\alpha > 0.7$). Mechanistic explanations based on "chain type" highly energetic reaction intermediates are discounted [2] because reactions readily resume after interruption with cooling [3]. The alternative reaction model, crack propagation followed by favoured product nucleation on exposed planes, accounts for the kinetic behaviour but is not positively supported by our electron micrographs. Crack propagation is not initiated from the outer crystal surfaces, which appear to be relatively inert. No patterns or alignments of internal disintegration related to crystallographic features could be discerned. If reaction proceeds by this mechanism, the textural features developed must be below the limits of microscopic resolution used here ($<0.05\,\mu$m) and/or subsequent product retexturing obliterates the details of crack development.

The accuracy of our measured α-time data is sufficiently precise to permit kinetic analyses based on consideration of the differential data, as in Fig. 7. It is evident from these plots, together with further similar data, that reaction is initiated relatively rapidly: the data do not extrapolate through the origin. Subsequent decomposition is acceleratory to $\alpha = 0.65 \pm 0.02$, the approximately constant maximum rate achieved is maintained thereafter $0.65 < \alpha < 0.80$ before the final deceleration to completion, $\alpha = 1.00$. This pattern of behaviour is not quantitatively or comprehensively represented by any one of those rate expressions that have found application in the kinetic analyses of reactions of solids [2]. Some conclusions may, however, be deduced from the form of the curves shown in Fig. 7.

Mechanism of decomposition

From the available evidence, we conclude that the most satisfactory mechanistic explanation for $CsMnO_4$ decomposition involves the intervention of a melt within which anion breakdown preferentially occurs. Reaction is expected to occur more readily in the molten phase because of

the absence of the constraining and stabilizing crystal forces [2]. Also the increased freedom of movement and disposition of participating ions enables them to adopt the configuration that minimizes the energy barrier to reaction. This molten phase arises through the formation of a reactant-product eutectic ($CsMnO_4 + Cs_2MnO_4$) which fuses at a lower temperature than either component. We note that no caesium analogue to the $K_3(MnO_4)_2$ phase is formed [8]. We regard this reaction model as providing the reason for the rounded features of intracrystalline material seen in Figs. 4(b) and 4(c), where the product is composed of aggregates of smaller grains that have apparently sintered together. These may be separate crystals of product Cs_2MnO_4 [8] and with other solid products present, possibly including MnO_2. Melting may be local (intracrystalline) and temporary but comprehensive liquefaction is prevented by the apparently unreactive external crystallite skin (see also ref. 7).

The initial rapid onset of reaction ($\alpha_i = 0.02$) is identified with surface decomposition, perhaps yielding the unreactive superficial layer, and other sites of enhanced reactivity usually identified [2] as crystal imperfections. The reaction products include Cs_2MnO_4 which is believed to melt with $CsMnO_4$. The direct proportionality between amount of product Cs_2MnO_4 and α explains the linear increase in rate in Fig. 7, $0.1 < \alpha < 0.65$, representing obedience to the exponential law [2] $(d\alpha/dt) = kt$ [7] or the Prout–Tompkins eqn. (1), as observed. Crushing the reactant with product (Fig. 8) increases the effective contact ($CsMnO_4 + Cs_2MnO_4$) so that the amount of molten eutectic formed soon after heating is increased, resulting in a corresponding rise in the reaction rate. The effects of pre-irradiation [5] are similar if it is assumed that this caused decomposition (and Cs_2MnO_4) within the crystal, which on heating yields local fusion sites from which reaction develops. This is consistent with the observed obedience [5] of decomposition of irradiated salt to the Prout–Tompkins equation and the observation that rate rises with dose. The activation energy is not changed by irradiation because the reaction mechanism is unaltered. Moreover, irradiated material undergoes explosive disintegration during subsequent reaction [5] due to intracrystalline retained product oxygen. The participation of melting also accounts for our observation that crushing the reactant did not increase the maximum rate of subsequent decomposition.

Activation energy values (in $kJ\,mol^{-1}$) for the decompositions of potassium (160 [3], 153 [11], 160 [12]), rubidium (160–166 [4]) and caesium (140–170 [3], 146 (this work)) permanganates were closely similar. This suggests that the constituent cations exert little (or no) influence in controlling reaction rate. It has also been noted [5] that the effects of irradiation on these decompositions is largely independent of the cations present. We conclude, therefore, that the decomposition of caesium permanganate is dominated by interactions between anions and therefore that the electron transfer step discussed by Boldyrev [6] satisfactorily

explains the observed behaviour

$$2MnO_4^- \rightarrow MnO_4^{2-} + MnO_4$$
$$\downarrow$$
$$\text{Products } (?MnO_2 + O_2)$$

In caesium permanganate we believe that the reaction proceeds in an intracrystalline fluid melt containing Cs^+ together with MnO_4^- and MnO_4^{2-} and that other products including MnO_2 and, later, Cs_2MnO_4 are precipitated. The decomposition rate is controlled by the amount of fused salt present because this constitutes the reaction medium. This progressively rises during the early stages of reaction, explaining the predominantly acceleratory character (Fig. 5) but later declines as the amount of permanganate remaining decreases.

ACKNOWLEDGMENT

We thank the staff of the Electron Microscope Unit of The Queen's University of Belfast for their help and advice in obtaining the electron micrographs. S.A.A. Mansour thanks the Egyptian Government for financial support.

REFERENCES

1 E.G. Prout and F.C. Tompkins, Trans. Faraday Soc., 40 (1944) 488.
2 M.E. Brown, D. Dollimore and A.K. Galwey, Comprehensive Chemical Kinetics, Vol. 22, Elsevier, Amsterdam, 1980.
3 P.J. Herley and E.G. Prout, J. Chem. Soc., (1959) 3300.
4 P.J. Herley and E.G. Prout, J. Inorg. Nucl. Chem., 16 (1960) 16.
5 E.G. Prout and P.J. Herley, J. Phys. Chem., 66 (1962) 961.
6 V.V. Boldyrev, J. Phys. Chem. Solids, 30 (1969) 1215.
7 N.J. Carr and A.K. Galwey, Proc. R. Soc. London Ser. A, 404 (1986) 101.
8 B.G. Erenburg, L.N. Senchenko, V.V. Boldyrev and A.V. Malysh, Russ. J. Inorg. Chem., 17 (1972) 1121.
9 A.K. Galwey and L. Pöppl, Philos. Trans. R. Soc. London Ser. A, 311 (1984) 159.
10 A.K. Galwey, N. Koga and H. Tanaka, J. Chem. Soc. Faraday Trans. 1, 86 (1990) 531.
11 R.A.W. Hill, R.T. Richardson and B.W. Rodger, Proc. R. Soc. London Ser. A, 291 (1966) 208.
12 M.E. Brown, K.C. Sole and M.W. Beck, Thermochim. Acta, 92 (1985) 149.